

New Hybrid HST Pump Development for Wave Energy Applications-Study on the Slipper Bearing of an Axial Piston Pump

S.D.G.S.P. Gunawardane^{#1}, Sudesh Ratnayake^{#2}, Tomiji Watabe^{*3}

[#]Dept. of Mechanical Engineering, Faculty of Engineering, University of Peradeniya, Peradeniya, Sri Lanka, 20400

¹sdgspg@eng.pdn.ac.lk, ²sudeshrathnayake@eng.pdn.ac.lk

^{*}T-Wave Consultant

5-23-3, Misono, Noboribetsu, 059-0036, Japan

³t1watabe@rg8.so-net.ne.jp

Abstract— Design of wave energy devices to withstand extreme conditions is a major challenge in wave energy development. Oscillating body devices use relative motion between the bodies to harness the energy though the motion limitation is necessary due to the motion restrictions of the power take off (PTO) mechanisms. This paper focuses on the development of an axial piston pump, which is an integral part of a new hydraulic PTO system that does not need motion restrictions. Since the axial piston pump rotates at relatively slow speed than typical speeds, the effect of lubrication at the motion transfer parts (mainly between swash plate and the slipper bearing) is the key focus of this study. Conventional groove design of the slipper bearing and proposed pocket design were studied and compared using analytical and CFD methods. It is found that, at very slow speeds, the new pocket design shows higher ability to maintain self-balancing on the lubrication layer than that of the conventional slipper bearing. Hence, new design has prospective for further development to enhance the lubrication ability at very slow speeds suitable for wave energy applications.

Keywords— HST, axial piston pump, Pendulor, slipper bearing, PTO,CFD

I. INTRODUCTION

Reliability and performance of any wave energy device highly depend on the robustness and the quality of the power takeoff system (PTO system). Premature failure of PTO system is one of the key reasons that hinder commercialization of leading wave energy concepts [1]. The cause of failures observed was mostly the shock loads and such incidences have been reported in for example Pendulor, Pelamis and Oyster [1]. It is noticeable that many of wave energy concepts, irrespective of their mode of oscillations, still prefer to use conventional piston cylinder hydraulic PTO systems. That is due to the simplicity and availability of the technology. The Pendulor device, which was invented almost forty years ago by Muroran Institute of Technology Japan, reported failures during sea trails mainly due shock loadings to the piston pump system. As a remedy, the piston pump system was replaced by rotary vane type to reduce such loadings and later many developments of such systems have been reported [2]. Recently, the floating version (Floating Pendulor) developed in Korea is on the verge of sea deployment in 2018 equipped with rotary vane type pump [1].

Still the research and development would be necessary before marking them fully ready for commercial operations.

In case of a flap device with a linear piston pump or a rotary vane pump, the system must have a stopper (active or passive) to limit amplitude of oscillations within the limits of the stroke of the pump. As a result, some components of the stopper are likely to damage frequently and the shock indirectly results fatigue failure in the other components as well. In order to avoid such failures, a new design strategy has been conceptualized without the use of stoppers [1]. This idea is named as Hybrid HST PTO system (shown in figure 1) which allows the flap to freely rotate around its own axis [1].

The simple concept of hybrid HST system is schematically shown in figure 1 together with the concept of the Pendulor device. A larger central gear transmits the flap motion via pinions to the axial piston pumps. Several number of axial piston pumps attached to the pinion deliver hydraulic fluid to the hydraulic motors to run the generator.

This paper mainly focuses on the development the axial piston pump particularly for very slow speed operations inherent to wave energy applications.

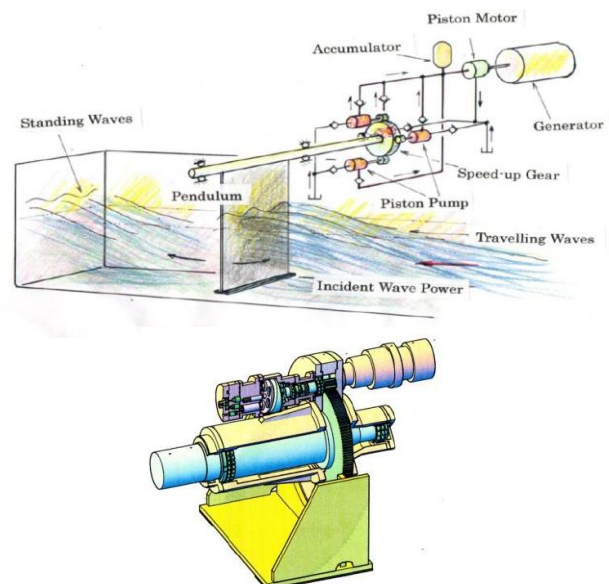


Figure 1(a) Concept of the new PTO system[1]

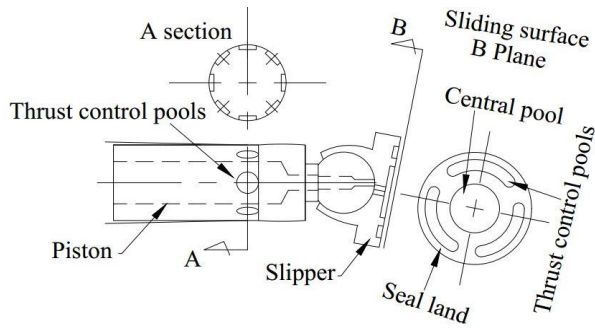


Figure 1(b). Concept of piston slipper unit (Japanese patent pending)

II. AXIAL PISTON PUMP AND LUBRICATION PROBLEM

Certain types of axial piston pumps/motors use swash plate to convert reciprocal motion to rotary motion. The intermediate element of that motion transfer is the slipper bearing and its performance is vital to reliable and efficient operation of the system. Therefore, the slipper bearing and the swash plate contacting behaviour (possible metal-metal contact) is critical for any kind of piston pump/motor. Iboshi and Ymaguchi developed theoretical analysis on the characteristics of the slipper bearing but these analyses were carried out for the single land slippers with central pocket [3]. They have derived several equations for forces and pressure distribution on the slipper land by making several assumptions to the Navier-Stokes equations of motion. Bergada et al [5], [6] derived series of equations for the pressure distribution and leakage of axial piston pump slipper with multiple lands. Kumar performed CFD characteristics of slipper bearing in collaboration with Bergada et al [6] considering the symmetrical grooved slipper. Juan chen, Jiming Ma, Jia Li, Yongling Fu have done the CFD analysis for the axial piston pump slipper bearing using COMSOL multiphysics [7] considering zero tilt angle of a conventional grooved slipper.

Previous studies [3][5][6] focused mainly on the cases of single land or grooved slippers with central pocket or sometimes behaviour of vented grooves in slippers. The focus of all those studies was for conventional applications of hydraulic pump/motor at relatively high speed of operations. On contrary, the pump speed is very slow in wave energy applications and hence the effectiveness of hydrodynamic lubrication action is expected to be low in the slipper bearings. The friction by probable metal contact at the slipper bearing and fair amount of oil leak could possibly make the condition worse. To the same reasons, the available designs of axial piston pumps will not fit well with this slow speed high torque application. Therefore, a new design concept introduced to the axial piston shoe design, which is expected to be superior in performance compared to commonly available design [6]. The novel design concept consists of thrust control pools at the ball joint end of the piston (not discussed in this paper) and multi pocket shoe as shown in Figure 1(b). The underline purpose of this thrust control pools and pocket design of the shoe is to provide adequate lubrication

to the sliding surfaces at relatively slow speeds and to provide adequate restoring moment to the slipper bearing at tilted condition (slipper stability). Thus, the primary objective of this study is to investigate the performance of conventional and new concept through the numerical modelling. The widely researched grooved design is taken as the base case [5][6][7].

III. ESTIMATION OF THE BASIC SHOE DIMENSION

There are substantial number of studies have been done to determine the behaviour of the slipper bearing in axial piston pumps [3][5][6]. Generally, pressure, leakage, thrust force and torque characteristics are derived to understand the slipper behaviour.

To determine the above characteristics, reasonable combination of slipper dimensions of the proposed design was found systematically. Figure 1(b) shows the schematic of the proposed design. Diameter of the piston is set to 2.5 cm (d_p) as the only known geometric parameter of the piston slipper combination [8]. Then by considering the equilibrium between piston force and reaction force on the slipper, equation 1 can be derived.

$$\frac{1}{4} d_p^2 P_p = r_a^2 P_s + r_1 w (P_s + P_c) + 2r_2 w_2 P_c + r_3 w_3 P_c \quad (1)$$

P_p is the inlet pressure, P_c and P_s are pressure of the central pocket and pressure of small pocket respectively. r and w values denote the radius and width values as shown in figure 2.

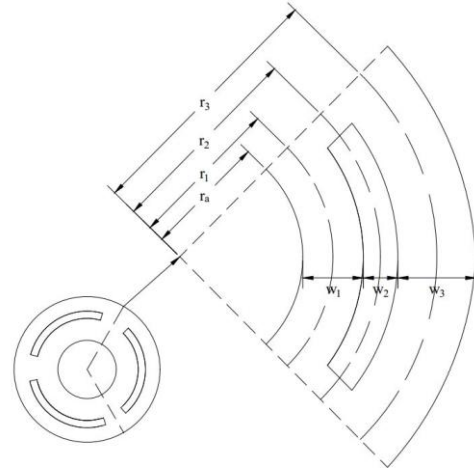


Fig. 2. Piston slipper dimensions

From equation 1, pressure P_s can be derived from pressure P_p ($P_c \approx P_p$) as well as w can be replaced using r . Therefore, equation 1 can be simplified to five independent variables, which are r_a , r_1 , r_2 , r_3 and d_p . Then r_a , r_1 , r_2 , r_3 and d_p should be obtained to satisfy the equilibrium within the suitable dimensions (MATLAB optimization and symbolic solver is used). Then, feasible dimensions of the novel slipper design are set as; $r_a = 0.7$ cm; $r_1 = 0.9$ cm; $r_2 = 1.2$ cm; $r_3 = 1.59$ cm.

Above dimensions are approximately similar to the conventional grooved slipper design with a central pocket used in [5] and [6]. Therefore, a fine comparison is possible between conventional and novel designs. Figure 3 shows the dimensions

used in this the study for both slipper configurations. The only difference in the novel design is the discontinuity of the circular groove and making it into three pockets. Please also note that, such a simple initial design considered for analytical easiness and studies are ongoing for more options.

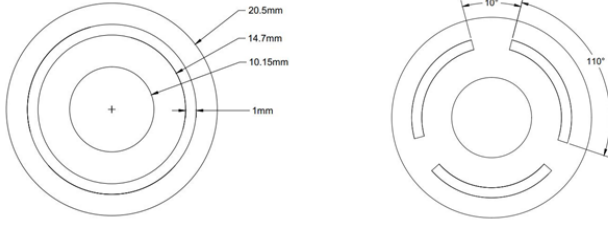


Fig. 3 slipper with single groove and three pockets designs.

IV. ANALYTICAL MODELLING

Reynold equation of lubrication, which is widely used in lubrication problems, is used in this study as well. Bergada et al[6] derived series of generalized equations for the pressure distribution on grooved slipper bearing using Reynolds equation of lubrication [4]. In this particular case, the slipper-bearing surface divided into two distinguish circle sectors as pocket portion and land portion(in between pockets). Similar derivations as per Bergada's approach used for the sectors that include pockets (the derived equations are not included in this paper since those equations are too long). Whereas, for the land part between pockets, the Reynolds equation of lubrication is used with suitable boundary conditions and assumptions. Throughout the analytical process, it is assumed that; the flow is laminar; the flow direction is radial only; static conditions; slipper pockets, groove, and slipper lands are flat.

For the derivation of pressure distribution in the land area, Reynold's equation of lubrication is used (shown in equation (2) with standard notations) [4]. Considering radial flow assumption and the static conditions, equation (3) and equation (4) are obtained.

$$\frac{1}{r} \frac{\partial(rh^3 \frac{\partial p}{\partial r})}{\partial r} + \frac{1}{r^2} \frac{\partial(h^3 \frac{\partial p}{\partial \theta})}{\partial \theta} = 6\mu \left[(U \cos \theta + V \sin \theta) \frac{\partial h}{\partial r} + (-U \sin \theta + V \cos \theta) \frac{\partial h}{r \partial \theta} + \frac{\partial h \omega}{\partial \theta} \right] \quad (2)$$

$$\frac{1}{r} \frac{\partial(rh^3 \frac{\partial p}{\partial r})}{\partial r} + \frac{1}{r^2} \frac{\partial(h^3 \frac{\partial p}{\partial \theta})}{\partial \theta} = 6\mu \left[(U \cos \theta) \frac{\partial h}{\partial r} + (-U \sin \theta) \frac{\partial h}{r \partial \theta} + \frac{\partial h \omega}{\partial \theta} \right] \quad (3)$$

$$\frac{1}{r} \frac{\partial(rh^3 \frac{\partial p}{\partial r})}{\partial r} = 6\mu \frac{\partial h \omega}{\partial \theta} \quad (4)$$

$$Q_{leakage} = \int_0^{2\pi} \int_0^h ur \, dy \, d\theta \quad (5)$$

Using equation (4) and flow rate equation (5), pressure distribution in the land area in between two pockets were derived. All derivations are based on the static conditions of the slipper. Then combining both pressure distributions in land and pocket areas, the total pressure distribution across the slipper was obtained.

V. CFD MODELLING

The lubrication layer between the swash plate and the slipper was modelled using Ansys Fluent CFD tool for further understanding and to compare with analytical results. Fluid domains in groove and the pocket design were analysed for zero tilt and maximum tilt. Comparable CFD analysis for slipper bearings could be found in some literature, but the focus of those had mostly on symmetrical designs with zero-tilt condition or for a portion of the slipper considering the symmetry [5][6][7].

In this study, CFD analysis was done for entire fluid domain for zero tilt angle as well as for maximum tilting condition. The critical areas of the fluid domain were discretised to hexahedral mesh to reduce the computational demand while maintain the accuracy by increasing the number of cells. The mesh patterns of the fluid domains are shown in figures 4 and 5.

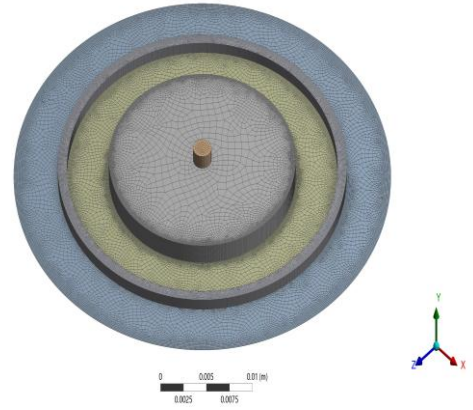


Fig. 4 Mesh for slipper with single groove

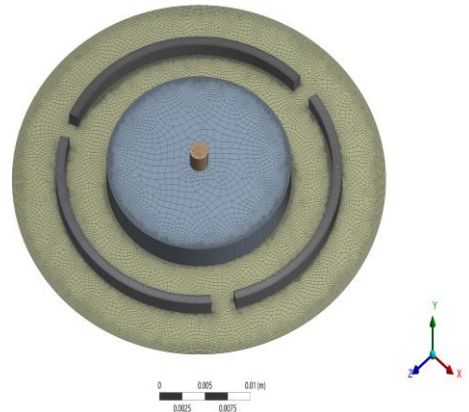


Fig. 5 Mesh for slipper with pockets

VI. RESULTS

For the current analysis it is assumed that the slipper is in static conditions and the system pressure (input pressure) is set to $P_p=10^7$ Pa and the output pressure $P_{out}=0$ Pa. The fluid viscosity is 0.032 Ns/m², maximum tilt angle relative to the swash plate surface is 0.03° deg and the clearance is 15 μ m. Dimensions of both configurations are shown in figure 3.

To make a reasonable comparison for the both conjunctions, input values or the reference values shown above were kept similar values as per some previous studies [5] [6]. Then pressure distribution and leakage were obtained for both groove and pocket designs. The following four cases are considered for the analysis.

1. Zero tilt for the pocket design.
2. Zero tilt for the grooved design
3. Maximum tilt for the pocket design.
4. Maximum tilt for the grooved design.

A. Slipper with zero tilt angle

Pressure distributions found through analytical process shown in figures 6 to 9 for both types of slippers. These plots contain 3D surface plots and 2D plots(across the diameter) as shown. The results show almost symmetrical pressure variations for both cases.

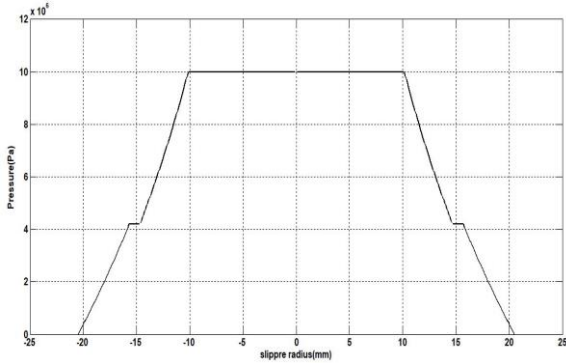


Fig. 6 Pressure variation across the diameter of grooved slipper

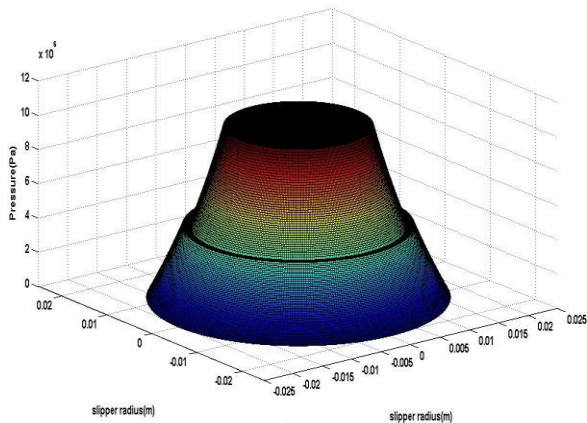


Fig. 7 Pressure variation across the diameter of grooved slipper surface plot

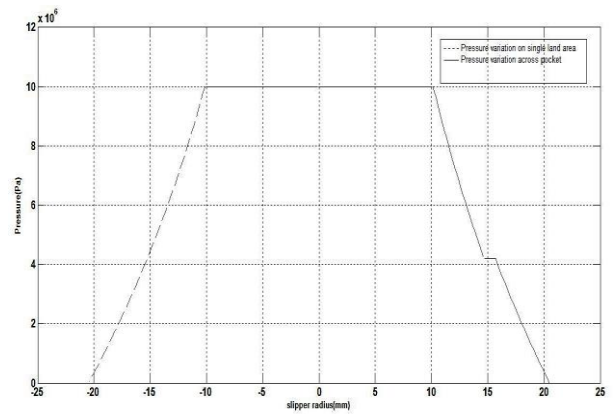


Fig. 8 Pressure variation along the diameter of pocket slipper

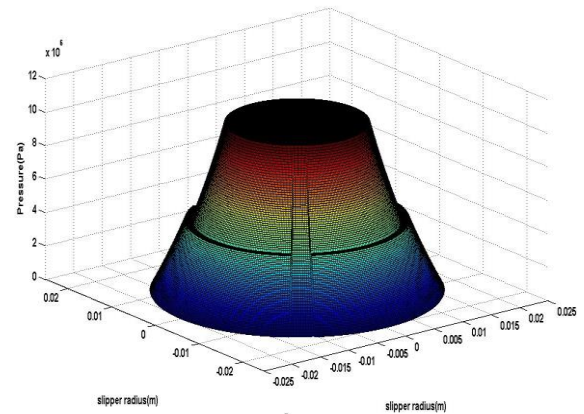


Fig. 9 Pressure variation across the diameter of pocket slipper surface plot

Under the same conditions, the pressure distributions were found using the CFD analysis. It is assumed that the slipper tilts around z axis and the origin of the coordinate system is at the slipper centre. Figures 10 and 11 show the pressure variation pattern for grooved slipper and pocket slipper respectively for zero tilt condition.

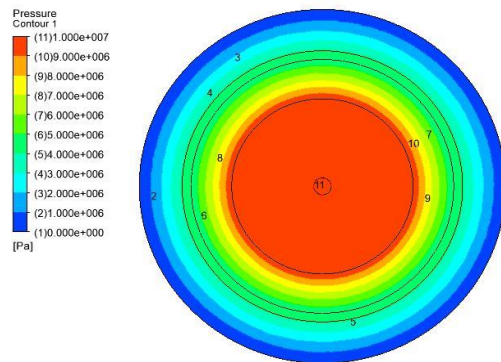


Fig 10. Pressure variation for grooved slipper at zero tilt position

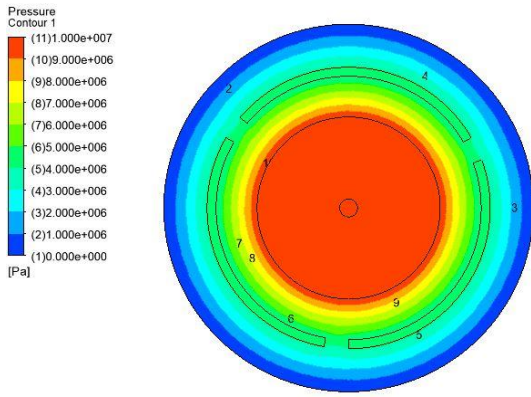


Fig. 11 Pressure variation for grooved slipper at zero tilt position

It is noticeable that the pressure distribution is almost symmetrical.

To compare the CFD results and the analytical results, pressure distributions along diameters of both designs (in pocket slipper, line goes across a pocket and land between two pockets) were considered. The analytical and CFD results are closely match for each case for zero tilt angle (Figures 6,8,12,13). Therefore, it is reasonable to assume that the methodology used for CFD is accurate enough for further analysis.

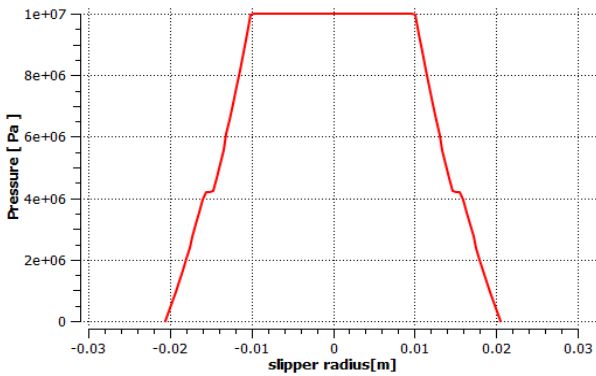


Fig. 12 Pressure variation across the diameter of grooved slipper (CFD)

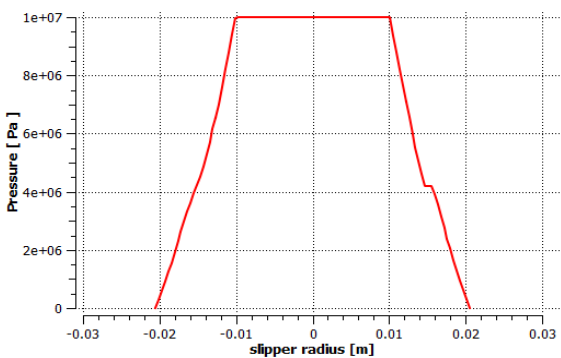


Fig. 13 Pressure variation across the diameter of pocket slipper surface (CFD)

B. Slipper with maximum tilt angle

To investigate the slipper characteristics under tilted conditions, similar analysis was performed by CFD. Figures 14

and 15 show the pressure distribution of groove and pocket designs respectively for maximum tilting condition. It is visible that the pressure distribution has a distinguish difference and that of the pocket design has a shift towards the pocket where the minimum gap is presence (See figure 15). Whereas, the shift of the pressure distribution is not very significant in the groove design.

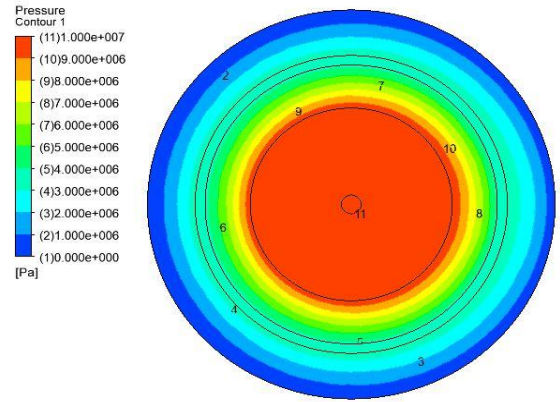


Fig. 14. Pressure variation for grooved slipper at max tilt angle

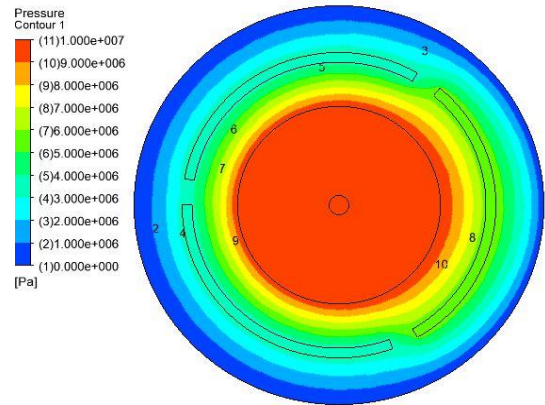


Fig. 15. Pressure variation for pocket slipper at max tilt angle

According to the defined coordinate system, the restoring moment applied on the slipper around z axis is also calculated. It is found that the restoring moment for the grooved design is 1.87 Nm and the same for the pocket design is 6.64 Nm.

C. Leakage comparison

Leakage in a well-designed and well-fabricated piston pumps are usually not a significant issue. Anyhow, in this endeavour, the leakages for both designs are compared. Figure 16 shows the analytically obtained leakage results with the tilting angle. It is visible that the leakage loss of the pocket design is slightly less than the groove design.

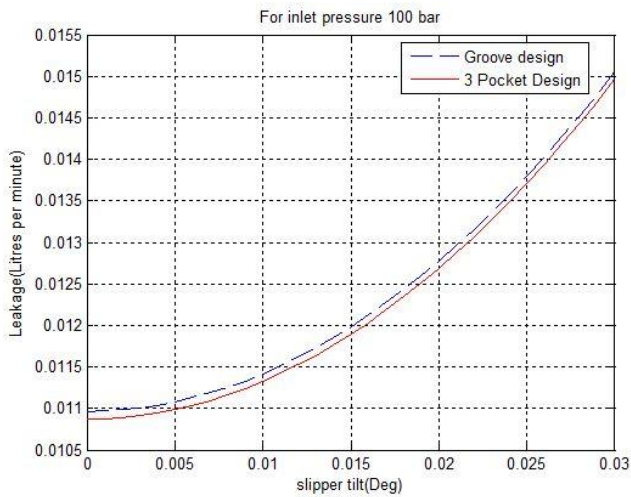


Fig 16. Leakage comparison of grove design and pocket design

However, the analytical results are based on several assumptions (2D flow) and the fluid flow diffraction at the edges of the pockets have not been accounted. Therefore, leakage losses calculated by CFD analysis is considered to be more reliable than that of the analytical results. Leakage of grooved and pocket designs were 52 ml/min and 51.9 ml/min respectively at zero tilting angle. At the maximum tilting angle condition, leakage of the grooved design was 72.3 ml/min and leakage for pocket design was 70.9 ml/min.

VII. DISCUSSION

Comparing the analytical and CFD results, pressure distribution for zero tilt angle shows similar results. Therefore, CFD analysis was considered reasonably accurate to further model the lubrication problem with tilted condition.

According to CFD analysis, the restoring moment on the slipper of the pocket design is three times greater than that of the grove design at the maximum tilt position (0.03 deg). Also, the leakage of the pocket design is slightly better than that of the grove design. For zero tilt position, both designs have the same thrust of 7.03 kN. In a previous study [1] a slipper of having high tendency to get larger restoring moment has been defined as a self-balancer. It means that the whenever the slipper happens to tilt with respect to the swashplate the fluid

pressure helps more in pocket design to make it un-tilt. Hence, according to the current findings we can conclude that the slipper with pockets has a greater self-balancing ability.

So far, the pocket design shows improvement for very slow operating conditions and further analysis are on the way to verify those more deeply. Therefore, as anticipated in the concept, the pocket design is more promising for further investigation. Further, studies are underway to investigate dynamic behavior of the slipper with different pocket configurations.

According to the experience of the current authors particularly on PTO system associated failures, the need of design standards/methodologies for wave energy device components is strongly felt. Therefore, more attention should be given to the design aspects of wave energy device components and this will open up more research and development opportunities.

ACKNOWLEDGMENT

Ms. C. Nagaishi for financial assistance to the study and Prof. Young-Ho Lee, Korea Maritime and Ocean University for conference facilitation.

REFERENCES

- [1] Tomiji WATABE, S.D.G.S.P. GUNAWARDANE, Wave power converter Pendulor with hybrid HST, Fluid Power JFPS International Symposium, October 2017.
- [2] Tomiji WATABE, Hirotaka YOKOUCHI, Hideo KONDO, Masaru INOYA, Mamoru KUDO "Improvement of rotary vane pump for an ocean wave power converter-Pendulor", Fluid Power. Forth JHPS International Symposium 1999
- [3] Naohiri IBOSHI, Atsushi YMAGUCHI, "Characteristics of a slipper bearing for swash plate type axial piston pumps and motors-1st report, theoretical analysis", JSME, Vol.25, No.210,1982.
- [4] Alastair Cameron, "The principles of lubrication". Published by Longman, chapter 3, pp 49-98, 1966.
- [5] J. M. Bergada, J. M. Haynes & J. Watton, "Leakage and Groove Pressure of an Axial Piston Pump Slipper with Multiple Lands", TribologyTransactions,51:4,469482,DOI:10.1080/10402000802044332, 2008
- [6] J.M.Bergada, S. Kumar, J.Watton, "Axial Piston Pumps-New Trends and Development",2012
- [7] Chen Juana, Ma Jimingb, Li Jia,Fu Yongling, "Performance optimization of grooved slippers for aero hydraulic pumps", Chinese Journal of Aeronautics,2015.

